

Summation-By-Parts Operators and High-Order Quadrature[☆]

J.E. Hicken^{a,1,*}, D.W. Zingg^{a,2}

^a*Institute for Aerospace Studies, University of Toronto, Toronto, Ontario, M3H 5T6, Canada*

Abstract

Summation-by-parts (SBP) operators are finite-difference operators that mimic integration by parts. The SBP operator definition includes a weight matrix that is used formally for discrete integration; however, the accuracy of the weight matrix as a quadrature rule is not explicitly part of the SBP definition. We show that SBP weight matrices are related to trapezoid rules with end corrections whose accuracy matches the corresponding difference operator at internal nodes. For diagonal weight matrices, the accuracy of SBP quadrature extends to curvilinear domains provided the Jacobian is approximated with the same SBP operator used for the quadrature. This quadrature has significant implications for SBP-based discretizations; in particular, the diagonal norm accurately approximates the L^2 norm for functions, and multi-dimensional SBP discretizations accurately approximate the divergence theorem.

Keywords: Summation-By-Parts operators, high-order quadrature, superconvergence, Euler-Maclaurin formula, Gregory rules

[☆]This work was supported by the Natural Sciences and Engineering Research Council (NSERC), the Canada Research Chairs program, Bombardier Aerospace, Mathematics of Information Technology and Complex Systems (MITACS), and the University of Toronto

*corresponding author

Email addresses: hickej2@rpi.edu (J.E. Hicken), dwz@oddjob.utias.utoronto.ca (D.W. Zingg)

¹Assistant Professor, Rensselaer Polytechnic Institute, Dept. of Mechanical, Aerospace, and Nuclear Engineering

²Professor and Director, Tier 1 Canada Research Chair in Computational Aerodynamics, J. Armand Bombardier Foundation Chair in Aerospace Flight

1. Introduction

Partial differential equations (PDEs) are often solved numerically in order to approximate a functional that depends on the solution; for example, when computational fluid dynamics is used to estimate the lift and drag on an aerodynamic body. For integral functionals, such as lift and drag, a quadrature rule is needed to numerically integrate the discrete solution. When we are free to choose the quadrature weights and abscissas, Gaussian quadrature is often the optimal choice. However, the choice of quadrature rule is less clear for the uniform grids that arise in finite-difference methods.

This paper highlights a quadrature rule that is particularly well suited for high-order summation-by-parts (SBP) finite-difference methods [8]. SBP operators lead to linearly time-stable discretizations of well-posed PDEs, and they have been used to construct efficient discretizations of the Euler [5, 11], Navier-Stokes [12–14], and Einstein equations [15]. The high-order quadrature in question is based on the weight matrix that forms part of the definition of SBP operators. This result is somewhat surprising, because the accuracy of the quadrature induced by the weight matrix is not explicitly part of the SBP definition. To our knowledge, the relationship between SBP operators and quadrature has not been discussed previously in the literature. The objective of this paper is to present this relationship and to demonstrate its importance.

In the context of high-order finite-difference methods, including those based on SBP operators, several classical quadrature rules are available to accurately evaluate integral functionals; for example, composite Newton-Cotes rules and Gregory-type formulae [7]. Why use a quadrature rule based on SBP weight matrices? While accuracy is important, we may also want the functional estimate to obey some property or properties of the true functional, and this is one attribute of SBP-based quadrature.

Consider the volume integral of the divergence of a vector field over a compact domain. The resulting functional is equivalent to the flux of the vector field over the domain's boundary, in light of the divergence theorem. This is a fundamental property of the functional that we may want a discretization and quadrature to preserve. We say a functional esti-

mate respects, or mimics, the divergence theorem if 1) it is accurate, and 2) the discrete quadrature over the volume produces a discrete quadrature over the surface.

In general, classical quadrature rules for uniformly spaced data will not mimic the divergence theorem in the above sense when applied to an arbitrary high-order finite-difference approximation of the divergence; typically, they will satisfy the first but not the second property. In contrast, we will show that a diagonal-norm SBP discretization does mimic the divergence theorem when numerically integrated using its corresponding weight matrix.

Another attractive property of SBP-based quadrature is that it can lead to superconvergent functionals. Specifically, given an $(s + 1)$ -order accurate solution of a dual-consistent diagonal-norm SBP discretization, $2s$ -order accurate integral functionals can be constructed using the SBP weight matrix [6]. The necessary role that SBP-based quadrature plays in these superconvergent functionals will be highlighted in the examples.

The paper is organized as follows. Section 2 introduces notation and formally defines SBP operators. Section 3 presents the main theoretical results. In particular, we derive conditions on the quadrature weights for the class of trapezoid rules with end corrections. These conditions are used to establish the accuracy of SBP-based quadrature. Subsequently, we consider the impact of coordinate transformations on diagonal-norm SBP quadrature and show that the quadrature remains accurate on curvilinear multi-dimensional domains. In Section 4 we verify the theoretical results with several numerical examples. The implications of SBP quadrature are summarized in Section 5.

2. Notation and definitions

We try to remain consistent with the notation used by Kreiss and Scherer in their original work [8], as well as Strand's subsequent work [17].

The interval $[0, 1]$ is partitioned into $n + 1$ evenly spaced points $x_v = vh$, $v = 0, 1, \dots, n$, with mesh spacing $h = 1/n$. Finite intervals other than $[0, 1]$, as well as nonuniform node spacing, can be accommodated by introducing an appropriate mapping (see Section 3.2). For arbitrary $\mathcal{U}(x) \in C^p[0, 1]$, we use $u_v = \mathcal{U}(x_v)$ to denote the restriction of \mathcal{U} to the grid x_v .

Definition 1 (Summation-By-Parts Operator). The matrix $D \in \mathbb{R}^{(n+1) \times (n+1)}$ is a summation-by-parts operator for the first derivative on the mesh $\{x_v\}_{v=0}^n$ if it has the form

$$D = H^{-1}Q,$$

where the weight matrix $H \in \mathbb{R}^{(n+1) \times (n+1)}$ is a symmetric-positive-definite matrix, and $Q \in \mathbb{R}^{(n+1) \times (n+1)}$ satisfies

$$Q + Q^T = \text{diag}(-1, 0, 0, \dots, 1).$$

Furthermore, the truncation error of the difference operator D in approximating d/dx is order h^{2s} at the internal nodes, $\{x_v\}_{v=r}^{n-r}$, and order h^τ at the boundary nodes, $\{x_v\}_{v=0}^{r-1}$ and $\{x_v\}_{v=n-r+1}^n$, where $\tau, r, s \geq 1$.

In other words, the SBP operator D approximates d/dx and has a particular structure. In general, the order of accuracy of the difference stencil at internal nodes is different than the order of accuracy of the stencil at boundary nodes. The even order of accuracy $2s$ for the internal nodes is a consequence of using centered-difference schemes, which provide the lowest error for a given stencil size. For a $2s$ -order accurate scheme, the derivative at the internal nodes is approximated as

$$\frac{d\mathcal{U}}{dx}(x_w) \approx \sum_{v=1}^s \frac{\alpha_v}{h} (u_{w+v} - u_{w-v}), \quad r \leq w \leq n-r,$$

where the coefficients are defined by (see [10], for example)

$$\alpha_v = \frac{(-1)^{v+1}(s!)^2}{v(s+v)!(s-v)!}.$$

The following lemma from [17] lists some identities that the α_v satisfy; these identities will be useful in our subsequent analysis.

Lemma 1. *The coefficients α_v that define a $2s$ -order accurate SBP operator at internal nodes satisfy*

$$\sum_{v=1}^s \alpha_v v^{2j+1} = \begin{cases} \frac{1}{2}, & j = 0, \\ 0, & j = 1, 2, \dots, s-1. \end{cases}$$

We turn our attention to the weight matrix H , which is the focus of this paper. Since H is symmetric-positive-definite, we can use it to define an inner product and corresponding norm for vectors. Let $u, z \in \mathbb{R}^{n+1}$ be two discrete functions on the grid nodes, i.e. $u_v = \mathcal{U}(x_v)$ and $z_v = \mathcal{Z}(x_v)$. Then

$$(u, z)_H \equiv u^T H z, \quad \text{and} \quad \|u\|_H^2 \equiv (u, u)_H,$$

define the H inner product and H norm, respectively. Using the SBP-operator definition and the H inner product, we have

$$(u, D z)_H = -(D u, z)_H - u_0 z_0 + u_n z_n. \quad (1)$$

Equation (1) expresses the fundamental property of SBP operators and is the discrete analog of

$$\int_a^b \mathcal{U} \frac{d\mathcal{Z}}{dx} dx = - \int_a^b \mathcal{Z} \frac{d\mathcal{U}}{dx} dx + \mathcal{U} \mathcal{Z} \Big|_{x=a}^{x=b}. \quad (2)$$

This property of SBP operators is what leads to energy-stable discretizations of partial differential equations. However, while (1) is analogous to integration by parts, it remains to be shown that (1) is an accurate discretization of (2).

In this work, we will consider H matrices with the block structure

$$H = h \begin{pmatrix} H_L & 0 & 0 \\ 0 & I & 0 \\ 0 & 0 & H_R \end{pmatrix}, \quad (3)$$

where $H_L, H_R \in \mathbb{R}^{r \times r}$ are symmetric-positive-definite matrices. Assuming that H_L and H_R are dense matrices — the so-called full-norm case — Kreiss and Scherer [8] established the existence of SBP operators that achieve an order of accuracy of $\tau = 2s - 1$ at the boundary with $r = 2s$. Strand [17] showed that $2s - 1$ accuracy can be maintained at the boundary in the case of a restricted-full norm, which uses

$$H_L = \begin{pmatrix} h_{00} & 0 \\ 0 & \bar{H}_L \end{pmatrix} \quad \text{and} \quad H_R = \begin{pmatrix} \bar{H}_R & 0 \\ 0 & h_{00} \end{pmatrix}$$

with $\bar{H}_L, \bar{H}_R \in \mathbb{R}^{(r-1) \times (r-1)}$ and $r = 2s + 1$.

In general, SBP weight matrices of the form (3) satisfy the compatibility conditions described in the following proposition [8]; these conditions will be used later to establish the accuracy of quadrature rules based on full and restricted-full H matrices.

Proposition 1. *Let $H \in \mathbb{R}^{(n+1) \times (n+1)}$ be an SBP weight matrix with the block structure (3).*

Then H_L satisfies

$$je_i^T H_L e_{j-1} + ie_j^T H_L e_{i-1} = -(-r)^{i+j} + J_{i,j}, \quad 0 \leq i, j \leq \tau,$$

where $e_j^T \equiv (-1)^j \begin{pmatrix} r^j & (r-1)^j & \dots & 1^j \end{pmatrix}$, with the convention $e_{-1} = 0$, and

$$J_{i,j} = \sum_{v=1}^s \alpha_v \left[\sum_{w=0}^{v-1} w^j (w-v)^i + w^i (w-v)^j \right], \quad i+j \geq 1.$$

Kreiss and Scherer also showed that it is possible to define SBP operators with diagonal H matrices, i.e.

$$H_L = \text{diag}(\lambda_0, \lambda_1, \dots, \lambda_{r-1})$$

$$H_R = \text{diag}(\lambda_{r-1}, \dots, \lambda_1, \lambda_0)$$

with $\lambda_i > 0$. These “diagonal norms” are important because, unlike full and restricted-full norms, they lead to provably stable PDE discretizations on curvilinear grids [18]. However, diagonal-norm SBP operators are limited to $\tau = s$ accuracy at the boundary when the internal accuracy is $2s$. Consequently, the solution accuracy of hyperbolic systems discretized with such SBP operators is limited to order $s + 1$ [4]. Nevertheless, one can show that functionals based on the solution of dual consistent diagonal-norm SBP discretizations are $2s$ -order accurate [6].

When the weight matrix H is diagonal, Kreiss and Scherer [8] showed that its elements are defined by the relations in following proposition.

Proposition 2. *Let $H \in \mathbb{R}^{(n+1) \times (n+1)}$ be a diagonal SBP weight matrix with $r = 2\tau = 2s$.*

Then the diagonal elements λ_v of H_L and H_R satisfy the relations

$$j \sum_{v=0}^{r-1} \lambda_v (r-v)^{j-1} = \begin{cases} (r)^j - (-1)^j \beta_j, & j = 1, 2, \dots, 2s-1 \\ (r)^{2s} - 2 \sum_{v=1}^s \alpha_v \sum_{w=0}^{v-1} w^s (w-v)^s, & j = 2s, \end{cases}$$

where β_j is the j^{th} Bernoulli number.

3. Theory

3.1. One-dimensional SBP Quadrature

To establish the accuracy of SBP-based quadratures, we need the following theorem that places constraints on the coefficients of a certain class of quadrature rules for uniformly spaced data; specifically, the trapezoid rule with end corrections. The theorem is a direct consequence of substituting finite-difference approximations into the Euler-Maclaurin sum formula.

Theorem 1. *Consider a set of $n+1$ uniformly spaced points, $x_v = vh$, $v = 0, 1, \dots, n$, with constant mesh spacing $h = 1/n$. A quadrature of the form*

$$\mathcal{I}(u) \equiv h \left(\sum_{v=0}^{r-1} \sigma_v u_v + \sum_{v=r}^{n-r} u_v + \sum_{v=0}^{r-1} \sigma_v u_{n-v} \right)$$

is a q -order accurate approximation of $\int_0^1 \mathcal{U} dx$ for $\mathcal{U} \in C^{2m+2}[0, 1]$, where $q - 1 \leq r$ and $q \leq 2m + 2$, if and only if the coefficients $\{\sigma_v\}_{v=0}^{r-1}$ satisfy

$$j \sum_{v=0}^{r-1} \sigma_v (r-v)^{j-1} = r^j - (-1)^j \beta_j, \quad j = 1, 2, \dots, q-1, \quad (4)$$

PROOF. Consider the Euler-Maclaurin sum formula applied to $\mathcal{U}(x)$ [7]:

$$\int_0^1 \mathcal{U}(x) dx = h \sum_{v=0}^n u_v + \sum_{k=1}^{2m} \frac{\beta_k}{k!} h^k \left(u_0^{(k-1)} - (-1)^k u_n^{(k-1)} \right) + E_{2m}, \quad (5)$$

where $u_v^{(k-1)} \equiv D^{(k-1)}\mathcal{U}(x_v)$, $2m < q \leq 2m + 2$, and the error term is given by

$$E_{2m} = \frac{\beta_{2m+2} h^{2m+2}}{(2m+2)!} D^{(2m+2)}\mathcal{U}(\xi),$$

with $\xi \in (0, 1)$. Suppose the function derivatives at $x = 0$ and $x = 1$ are replaced with finite-difference approximations involving the first r and last r internal points, respectively. Moreover, assume that the approximation to $u_v^{(k-1)}$ is accurate to $O(h^{q-k})$, where $q - 1 \leq r$;

consequently, the approximations are exact for polynomials up to at least degree $q - 1$. Let $\{\delta_v^{(k-1)}\}_{v=0}^{r-1}$ denote the coefficients defining the finite-difference approximation of $u_0^{(k-1)}$, such that

$$u_0^{(k-1)} = \sum_{v=0}^{r-1} \frac{\delta_v^{(k-1)}}{h^{k-1}} u_v + O(h^{q-k}).$$

Substituting the finite-difference approximations into (5), and noting that the coefficients for odd derivatives must be negated at $x = 1$, we find

$$\begin{aligned} \int_0^1 \mathcal{U}(x) dx &= h \sum_{v=0}^n u_v + \sum_{k=1}^{2m} \frac{\beta_k}{k!} h^k \sum_{v=0}^{r-1} \frac{\delta_v^{(k-1)}}{h^{k-1}} (u_v + u_{n-v}) + O(h^q) + O(h^{2m+2}) \\ &= h \left(\sum_{v=0}^{r-1} \sigma_v u_v + \sum_{v=r}^{n-r} u_v + \sum_{v=0}^{r-1} \sigma_v u_{n-v} \right) + O(h^q) \end{aligned}$$

where

$$\sigma_v = 1 + \sum_{k=1}^{2m} \frac{\beta_k}{k!} \delta_v^{(k-1)}, \quad v = 0, 1, \dots, r-1. \quad (6)$$

Next, we will show that these σ_v are the same ones that satisfy (4), a set of $q - 1$ conditions that are independent of the $\delta_v^{(k)}$. Substituting the above expression for σ_v into (4), we find

$$\begin{aligned} j \sum_{v=0}^{r-1} \sigma_v (r-v)^{j-1} &= j \sum_{v=0}^{r-1} (r-v)^{j-1} + j \sum_{k=1}^{2m} \frac{\beta_k}{k!} \sum_{v=0}^{r-1} \delta_v^{(k-1)} (r-v)^{j-1}, \\ & \qquad \qquad \qquad j = 1, 2, \dots, q-1. \quad (7) \end{aligned}$$

The first term on the right-hand side can be recast using the sum of powers formula³:

$$j \sum_{v=0}^{r-1} (r-v)^{j-1} = r^j + \sum_{k=1}^{j-1} (-1)^k \binom{j}{k} \beta_k r^{j-k}. \quad (8)$$

For the second term, we recognize that $(r-v)^{j-1}$ is the discrete representation of the polynomial $p_{j-1}(x) \equiv h^{-(j-1)}(rh-x)^{j-1}$; therefore, since the finite-difference approximations are exact for polynomials of degree $q - 1$, we have

$$\sum_{v=0}^{r-1} \delta_v^{(k-1)} (r-v)^{j-1} = \begin{cases} (-1)^{k-1} \frac{(j-1)!}{(j-k)!} r^{j-k}, & k \leq j \\ 0, & k > j, \end{cases}$$

³We use the sum of powers formula that is consistent with $\beta_1 = -\frac{1}{2}$

and

$$j \sum_{k=1}^{2m} \frac{\beta_k}{k!} \sum_{v=0}^{r-1} \delta_v^{(k-1)} (r-v)^{j-1} = \sum_{k=1}^j (-1)^{k-1} \binom{j}{k} \beta_k r^{j-k}. \quad (9)$$

Substituting (8) and (9) into (7), and recalling that the odd Bernoulli numbers greater than one are zero, we have

$$\begin{aligned} j \sum_{v=0}^{r-1} \sigma_v (r-v)^{j-1} &= r^j + \sum_{k=1}^{j-1} (-1)^k \binom{j}{k} \beta_k r^{j-k} + \sum_{k=1}^j (-1)^{k-1} \binom{j}{k} \beta_k r^{j-k} \\ &= r^j - (-1)^j \beta_j, \end{aligned}$$

for $j = 1, 2, \dots, q-1$. Thus, we have shown that the σ_v satisfy (4) when the quadrature is q -order accurate.

We need the general solution of (4) to show that these conditions are sufficient for the quadrature to be q -order accurate. We have already shown that (6) is a particular solution of the linear equations (4), so we need to determine the form of the homogeneous solution, i.e. the null space of the matrix on the left side of (4).

As noted above, $(r-v)^{j-1}$ is simply the polynomial $p_{j-1}(x) = h^{-(j-1)}(rh-x)^{j-1}$ evaluated at the nodes. The derivative operator $D^{(k-1)}$ with $q \leq k \leq r$ will annihilate $p_{j-1}(x)$, since $j \leq q-1$; therefore, any finite difference approximation that is a consistent approximation of $h^{k-1}D^{(k-1)}$, $q \leq k \leq r$, will annihilate $p_{j-1}(x_v) = (r-v)^{j-1}$. If we let $\{\mu_v^{(k-1)}\}_{v=0}^{r-1}$ denote the coefficients of such a finite difference approximation, then the general solution to (4) can be written as

$$\sigma_v = 1 + \sum_{k=1}^{2m} \frac{\beta_k}{k!} \delta_v^{(k-1)} + \sum_{k=q}^r \gamma_{k-q} \mu_v^{(k-1)}, \quad (10)$$

where $\{\gamma_0, \gamma_1, \dots, \gamma_{r-q}\}$ parameterizes the null space. When $r = q-1$, the null space is trivial, and the second sum does not appear in (10).

Substituting the general solution into the quadrature yields

$$\begin{aligned}
\mathcal{I}(u) &= h \left(\sum_{v=0}^{r-1} \sigma_v u_v + \sum_{v=r}^{n-r} u_v + \sum_{v=0}^{r-1} \sigma_v u_{n-v} \right) \\
&= h \sum_{v=0}^n u_v + \sum_{k=1}^{2m} \frac{\beta_k}{k!} h^k \sum_{v=0}^{r-1} \frac{\delta_v^{(k-1)}}{h^{k-1}} (u_v + u_{n-v}) \\
&\quad + h \sum_{k=q}^r \gamma_{k-q} \sum_{v=0}^{r-1} \mu_v^{(k-1)} (u_v + u_{n-v}) \\
&= \int_0^1 \mathcal{U}(x) dx + O(h^q) + \sum_{k=q}^r \gamma_{k-q} h^k \left(u_0^{(k-1)} + (-1)^k u_n^{(k-1)} \right) \\
&= \int_0^1 \mathcal{U}(x) dx + O(h^q).
\end{aligned}$$

Therefore, we have shown that (4) is sufficient for the quadrature to be q -order accurate, which completes the proof. \square

If we choose $q - 1 = r$, Theorem 1 provides a closed set of equations for constructing high-order quadrature rules for uniformly spaced data with equal weights on the internal points. More generally, we may choose $q - 1 < r$, in which case the additional degrees of freedom can be used to achieve other objectives. For example, setting σ_0 to zero, so that only strictly internal points are used.

Theorem 1 encompasses many existing quadrature rules, including the Gregory class of formulae (see, e.g., [7]), and it could be used to construct an unlimited number of novel trapezoid rules with end corrections. However, our interest in Theorem 1 is not in constructing new quadrature rules, but in its consequences for SBP weight matrices.

Corollary 1. *Let H be a full, restricted-full, or diagonal weight matrix from an SBP first-derivative operator $D = (H^{-1}Q)$, which is a $2s$ -order-accurate approximation to d/dx in the interior. Then the H matrix constitutes a $2s$ -order-accurate quadrature for integrands $\mathcal{U} \in C^{2s}$.*

PROOF. For diagonal SBP weight matrices the result follows immediately from Proposition 2, since (4), with $q = 2s$, is a subset of the equations that define the λ_v . For the full and

restricted-full weight matrices, consider the relations in Proposition 1 with $j \leq \tau = 2s - 1$ and $i = 0$:

$$j \sum_{v=0}^{r-1} \sum_{w=0}^{r-1} h_{vw} (-1)^{j-1} (r-w)^{j-1} = -(-r)^j + \sum_{v=1}^s \alpha_v \sum_{w=0}^{v-1} [w^j + (w-v)^j].$$

Multiplying the left and right sides by $(-1)^{j-1}$, using the symmetry of the h_{vw} , and swapping summation indices on the left side, we find

$$j \sum_{v=0}^{r-1} \sigma_v (r-v)^{j-1} = r^j + (-1)^{j-1} \sum_{v=1}^s \alpha_v \sum_{w=0}^{v-1} [w^j + (w-v)^j],$$

where σ_v is identified with $\sum_{w=0}^{r-1} h_{vw}$. The second term on the right-hand side can be simplified using the accuracy conditions of the α_v (Lemma 1) and the formula for the sum of powers.

$$\begin{aligned} \sum_{v=1}^s \alpha_v \sum_{w=0}^{v-1} [w^j + (w-v)^j] &= \sum_{v=1}^s \alpha_v \left[-v^j + \sum_{w=1}^v w^j + (-1)^j \sum_{w=1}^v w^j \right] \\ &= \sum_{v=1}^s \alpha_v \left[-v^j + \frac{(1 + (-1)^j)}{j+1} \sum_{w=0}^j \binom{j+1}{w} \beta_w v^{j+1-w} \right] \\ &= \begin{cases} -\frac{1}{2}, & j = 1 \\ 0, & j = 3, 5, \dots, \tau, \\ \beta_j, & j = 2, 4, \dots, \tau - 1 \end{cases} \\ &= \beta_j. \end{aligned}$$

Thus, we have

$$j \sum_{v=0}^{r-1} \sigma_v (r-v)^{j-1} = r^j - (-1)^j \beta_j, \quad 1 \leq j \leq \tau,$$

and Theorem 1 implies that full and restricted-full SBP weight matrices are quadrature rules accurate to $\tau + 1 = 2s$. \square

3.2. Diagonal-norm SBP Quadrature and Coordinate Transformations

Curvilinear coordinate systems are often necessary when solving PDEs on complex domains. Like most finite-difference schemes, SBP operators are not applied directly to the

nodes in physical space. Instead, a coordinate transformation is used to map points in the physical domain to points on a Cartesian grid, and the SBP operators are applied in this uniform computational space. However, this coordinate transformation introduces geometric terms whose impact on the accuracy of the quadrature rule is not clear. As we show below, the quadrature accuracy is indeed retained for diagonal SBP weight matrices.

We begin by considering the one-dimensional case. Let $\mathcal{T}(x) = \xi(x)$ be an invertible transformation of class C^{2s} that maps $\Omega_x = [a, b]$ to $\Omega_\xi = [0, 1]$. For $\mathcal{U} \in L^2(\Omega_x)$, the change of variable theorem implies

$$\int_a^b \mathcal{U} dx = \int_0^1 \mathcal{U} \mathcal{J} d\xi, \quad (11)$$

where $\mathcal{J} = \frac{dx}{d\xi}$ is the Jacobian of \mathcal{T}^{-1} .

We are interested in the accuracy of diagonal-norm SBP quadrature in the computational domain, so we consider the discrete equivalent of the right-hand side of (11). In general the mapping will not be explicitly available, so the Jacobian must be approximated. As we shall see, to retain the $2s$ -order accuracy of SBP quadrature, it is critical that the derivative that appears in the Jacobian be approximated by the same SBP difference operator that defines the norm. Thus, if $x \in \mathbb{R}^{n+1}$ denotes the coordinates of the nodes in physical space, the SBP approximation of (11) is given by

$$u^T H D x = u^T Q x. \quad (12)$$

The following theorem confirms that this discrete product is a $2s$ -order accurate approximation of the integral (11).

Theorem 2. *Let $D = H^{-1}Q$ be an SBP first derivative operator with a diagonal weight matrix. Then*

$$(z, Du)_H = z^T Q u$$

is a $2s$ -order-accurate approximation to the integral

$$\int_0^1 \mathcal{Z} \frac{d\mathcal{U}}{dx} dx,$$

where $\mathcal{Z} \frac{d\mathcal{U}}{dx} \in C^{2s}[0, 1]$.

PROOF. Using SBP-norm quadrature we have

$$\int_0^1 \mathcal{Z} \frac{d\mathcal{U}}{dx} dx = (z, u')_H + O(h^{2s}),$$

where u' denotes the analytical derivative $\partial\mathcal{U}/\partial x$ evaluated at the grid nodes. The result will follow if we can show that

$$(z, u')_H = (z, Du)_H + O(h^{2s}). \quad (13)$$

The expression on the left of (13) is simply a quadrature for the integrand $\mathcal{Y} = \mathcal{Z} \frac{d}{dx} \mathcal{U}$. Consequently, it is sufficient to show (13) is exact for polynomial integrands of degree less than $2s$. Let

$$w_i = [x_0^i \quad x_1^i \quad \cdots \quad x_n^i]^T$$

be the restriction of the monomial x^i to the grid. We will consider

$$z = w_i, \quad u = w_j, \quad \text{and} \quad u' = jw_{j-1},$$

with $i + j \leq 2s$.

First, suppose $j \leq s$. In this case, the SBP operator is exact for w_j giving

$$Du = Dw_j = jw_{j-1} = u',$$

and substitution into (13) yields $(z, u')_H = (z, Du)_H$.

Next, to show that (13) is exact for $j > s$, the roles of z and u will be reversed. Here, since $j + i \leq 2s$, we must have $i < s$, and the SBP operator becomes exact for w_i :

$$Dz = Dw_i = iw_{i-1} = z'.$$

Using this exact derivative and the properties of SBP operators we find

$$\begin{aligned}
(z, Du)_H &= z^T H(H^{-1}Q)u \\
&= z_n u_n - z_0 u_0 - z^T Q^T u \\
&= \mathcal{U}\mathcal{Z}|_{x=1} - \mathcal{U}\mathcal{Z}|_{x=0} - (u, Dz)_H \\
&= \mathcal{U}\mathcal{Z}|_{x=1} - \mathcal{U}\mathcal{Z}|_{x=0} - (u, z')_H \\
&= \int_0^1 \frac{d}{dx} (\mathcal{U}\mathcal{Z}) dx - \int_0^1 \mathcal{U} \frac{d\mathcal{Z}}{dx} dx \\
&= \int_0^1 \mathcal{Z} \frac{d\mathcal{U}}{dx} dx.
\end{aligned}$$

Thus we have shown that the expression $(z, Du)_H$ is also equal to the exact integral when $j > s$ and $i + j \leq 2s$. This completes the proof. \square

For multidimensional problems on curvilinear tensor-product domains, SBP operators are obtained from the one-dimensional operators using Kronecker products. To extend diagonal-norm SBP quadrature to these domains, we need only apply Theorem 2 iteratively over the individual coordinate directions. We provide a sketch of the proof here and direct the interested reader to [6] for the details of the two-dimensional case. Consider the change of variable theorem in d dimensions:

$$\int_{\Omega_x} \cdots \int \mathcal{W} dx_1 dx_2 \cdots dx_d = \int_{\Omega_\xi} \cdots \int \mathcal{W}\mathcal{J} d\xi_1 d\xi_2 \cdots d\xi_d,$$

where \mathcal{J} is the Jacobian of the mapping (more precisely, the determinant of the Jacobian). As in the one-dimensional case, the mapping and integrand must be sufficiently differentiable (class C^{2s}) for the quadrature to remain $2s$ -order accurate. An important observation is that the Jacobian consists of a sum of terms of the form

$$\frac{\partial x_i}{\partial \xi_1} \frac{\partial x_j}{\partial \xi_2} \cdots \frac{\partial x_k}{\partial \xi_d}$$

in which none of the indices i, j, \dots, k are equal. Because the indices of the computational coordinates are also distinct, Theorem 2 can be applied one dimension at a time (i.e., as an

iterated integral). For example, we can consider dimension ξ_1 and apply Theorem 2 to the integral

$$\int_0^1 \left(\mathcal{W} \frac{\partial x_j}{\partial \xi_2} \dots \frac{\partial x_k}{\partial \xi_d} \right) \frac{\partial x_i}{\partial \xi_1} d\xi_1,$$

where x_i corresponds with \mathcal{U} in the theorem, and

$$\left(\mathcal{W} \frac{\partial x_j}{\partial \xi_2} \dots \frac{\partial x_k}{\partial \xi_d} \right)$$

corresponds with \mathcal{Z} . Repeating this process over the remaining coordinate directions and terms in the Jacobian yields the desired result.

3.3. Diagonal-norm SBP Operators and the Divergence Theorem

Using the above results, one can show that SBP operators with diagonal weight matrices mimic the d -dimensional divergence theorem to order h^{2s} on curvilinear domains that are diffeomorphic to the d -cube. We will consider the two-dimensional case; the extension to higher dimensions is straightforward.

In two-dimensions, the divergence theorem is

$$\iint_{\Omega_x} \frac{\partial \mathcal{F}}{\partial x} + \frac{\partial \mathcal{G}}{\partial y} dx dy = \oint_{\partial \Omega_x} (\mathcal{F} dy - \mathcal{G} dx) \quad (14)$$

where $\partial \Omega_x$ is the piecewise-smooth boundary of Ω_x , oriented counter-clockwise. Applying the coordinate transformation, we find

$$\begin{aligned} \iint_{\Omega_x} \frac{\partial \mathcal{F}}{\partial x} + \frac{\partial \mathcal{G}}{\partial y} dx dy &= \iint_{\Omega_\xi} \left(\frac{\partial \mathcal{F}}{\partial x} + \frac{\partial \mathcal{G}}{\partial y} \right) \mathcal{J} dx dy \\ &= \iint_{\Omega_\xi} \frac{\partial \hat{\mathcal{F}}}{\partial \xi} + \frac{\partial \hat{\mathcal{G}}}{\partial \eta} d\xi d\eta \end{aligned} \quad (15)$$

where we have used the metric relations [16, 19] to obtain the components

$$\hat{\mathcal{F}} = \mathcal{J} \left(\frac{\partial \xi}{\partial x} \mathcal{F} + \frac{\partial \xi}{\partial y} \mathcal{G} \right) = \frac{\partial y}{\partial \eta} \mathcal{F} - \frac{\partial x}{\partial \eta} \mathcal{G}, \quad (16)$$

$$\hat{\mathcal{G}} = \mathcal{J} \left(\frac{\partial \eta}{\partial x} \mathcal{F} + \frac{\partial \eta}{\partial y} \mathcal{G} \right) = -\frac{\partial y}{\partial \xi} \mathcal{F} + \frac{\partial x}{\partial \xi} \mathcal{G}. \quad (17)$$

In light of (15), we need only show that diagonal-norm SBP discretizations obey the divergence theorem to order h^{2s} in the simpler computational space:

$$\iint_{\Omega_\xi} \frac{\partial \hat{\mathcal{F}}}{\partial \xi} + \frac{\partial \hat{\mathcal{G}}}{\partial \eta} d\xi d\eta = \int_0^1 [\hat{\mathcal{F}}(1, \eta) - \hat{\mathcal{F}}(0, \eta)] d\eta + \int_0^1 [\hat{\mathcal{G}}(\xi, 1) - \hat{\mathcal{G}}(\xi, 0)] d\xi. \quad (18)$$

The reader may object to this simplification, since $\hat{\mathcal{F}}$ and $\hat{\mathcal{G}}$ contain derivatives that depend on the geometry and must be approximated. However, if the partial derivatives of x and y appearing in (16) and (17) are approximated using the same SBP operators as found in the discrete divergence theorem, then Theorem 2 can be applied. This follows because the same difference operator is never applied twice in the same coordinate direction (e.g., $\partial/\partial\xi$ is applied to $\hat{\mathcal{F}}$, which contains only partial derivatives with respect to η).

For simplicity, assume that the square Ω_ξ is discretized using $n + 1$ nodes in both the ξ and η directions. Thus, the nodal coordinates are given by

$$\boldsymbol{\xi}_{jk} = (\xi_j, \eta_k) = \frac{1}{n}(j, k), \quad 0 \leq j, k \leq n\}.$$

If the nodes are ordered first by j and then by k , one-dimensional SBP operators can be used to construct the two-dimensional difference operators

$$D_\xi = (I \otimes D), \quad \text{and} \quad D_\eta = (D \otimes I),$$

where \otimes denotes the Kronecker product, $D = H^{-1}Q$ is the one-dimensional SBP operator, and I is the $(n + 1) \times (n + 1)$ identity matrix. Similarly, $(H \otimes H)$ defines the SBP quadrature for the two-dimensional set of points. Let $B = \text{diag}(-1, 0, 0, \dots, 1)$, so that we may write $Q + Q^T = B$. Finally, let \hat{f} and \hat{g} denote the restriction of the functions $\hat{\mathcal{F}}$ and $\hat{\mathcal{G}}$, respectively, to the grid points, and let $c = [1 \ 1 \ \dots \ 1]^T$ denote the constant function 1 restricted to the grid.

With the two-dimensional SBP operators suitably defined, we can discretize the left-hand

side of (18):

$$\begin{aligned}
c^T(H \otimes H) \left[(I \otimes D)\hat{f} + (D \otimes I)\hat{g} \right] &= c^T(H \otimes Q)\hat{f} + c^T(Q \otimes H)\hat{g} \\
&= c^T(H \otimes (B - Q^T))\hat{f} + c^T((B - Q^T) \otimes H)\hat{g} \\
&= \sum_{j=0}^n h_{ii}(\hat{f}_{n,j} - \hat{f}_{0,j}) + \sum_{i=0}^n h_{ii}(\hat{g}_{i,n} - \hat{g}_{i,0}), \quad (19)
\end{aligned}$$

where we have used $c^T(Q^T \otimes H) = c^T(H \otimes Q^T) = 0$ (constants are in the null space of $D = H^{-1}Q$).

We highlight two significant facts regarding (19).

1. It is a $2s$ -order accurate approximation of the right-hand side of (18).
2. It depends only on the terms of \hat{f} and \hat{g} that fall on the boundary.

Constructing a scheme that satisfies either one of these properties may not be difficult; however, few high-order schemes satisfy both 1 and 2 simultaneously. This is what we mean when we say the SBP operator mimics the divergence theorem.

4. Examples

4.1. One-dimensional Quadrature

To illustrate the basic theory, we use the weight matrices from several common SBP operators to integrate a simple function. We consider three SBP operators with diagonal weight matrices and one SBP operator with a full norm. The diagonal operators are taken from Diener *et al.* [2] and are denoted by $\text{diag-}\tau\text{-}2s$, where τ and $2s$ indicate the truncation error at the boundary and interior, respectively. The full norm operator can be found in [17] and is denoted $\text{full-}\tau\text{-}2s$. The boundary weights σ_v for all four operators are listed in Table 1; for the diagonal norms $\sigma_v = \lambda_v$, whereas for the full norm $\sigma_v = \sum_{w=0}^{r-1} h_{vw}$.

Table 1: Boundary quadrature weights corresponding to some SBP weight matrices.

SBP operator	τ	$2s$	σ_0	σ_1	σ_2	σ_3	σ_4	σ_5
diag-1-2 [†]	1	2	$\frac{1}{2}$	—	—	—	—	—
diag-2-4	2	4	$\frac{17}{48}$	$\frac{59}{48}$	$\frac{43}{48}$	$\frac{49}{48}$	—	—
full-3-4	3	4	$\frac{43}{144}$	$\frac{67}{48}$	$\frac{35}{48}$	$\frac{155}{144}$	—	—
diag-3-6	3	6	$\frac{13649}{43200}$	$\frac{12013}{8640}$	$\frac{2711}{4320}$	$\frac{5359}{4320}$	$\frac{7877}{8640}$	$\frac{43801}{43200}$

[†] the trapezoidal rule

Consider the definite integral

$$\begin{aligned}
 \mathcal{I} &= \int_0^1 \mathcal{U}(x) dx \\
 &= \int_0^1 (4\pi)^2 x \cos(4\pi x) dx \\
 &= -4\pi \cos(4\pi).
 \end{aligned} \tag{20}$$

To assess the accuracy of the SBP quadrature rules in Table 1, we perform a grid refinement study based on the integral (20) and using $n \in \{16, 32, 64, 128, 256, 512\}$. Table 2 lists the rates of convergence for the quadrature rules. For $n > 16$, the rate of convergence is calculated from

$$q_n = \frac{1}{\ln(2)} \ln \left(\frac{|E_{\frac{n}{2}}|}{|E_n|} \right), \tag{21}$$

where $E_n = \mathcal{I} - c^T H u$, with $c^T \equiv (1 \ 1 \ \dots \ 1)$, is the error using $n + 1$ nodes. In all cases, the errors converge to zero at the expected asymptotic rate of $2s$.

Figure 1 plots the errors E_n versus a normalized mesh spacing. This figure reminds us that schemes with the same order of accuracy can produce different absolute errors: the diag-2-4 operator is almost an order of magnitude more accurate than the full-3-4 operator for $n \geq 64$. This is surprising considering that the derivative operator corresponding to the full-3-4 norm has a truncation error that is $O(h^3)$ at the boundary while the derivative operator corresponding to the diag-2-4 norm is $O(h^2)$ at the boundary. However, further

Table 2: Rates of convergence for the SBP quadrature rules in Table 1 applied to (20).

SBP operator	n				
	32	64	128	256	512
diag-1-2	2.0113	2.0028	2.0007	2.0002	2.0000
diag-2-4	4.4978	4.4148	4.2182	4.1019	4.0473
full-3-4	4.1973	2.9369	3.7072	3.8876	3.9510
diag-3-6	5.7050	6.8942	6.9378	6.7651	6.5472

analysis is required before we can characterize the relative performance of these quadrature schemes more generally.

4.2. Multi-dimensional Quadrature on a Curvilinear Domain

As shown in Section 3.2, diagonal-norm SBP quadrature retains its theoretical accuracy on curvilinear domains provided the Jacobian of the transformation is approximated using the corresponding SBP difference operator. To verify this, we consider the domain

$$\Omega_x = \{(x, y) \in \mathbb{R}^2 \mid 1 \leq xy \leq 3, 1 \leq x^2 - y^2 \leq 4\},$$

and the integral

$$\begin{aligned} \mathcal{I} &= \iint_{\Omega_x} (x^2 + y^2) e^{\frac{1-x^2+y^2}{3}} \sin\left(\frac{xy-1}{2}\right) dx dy \\ &= 3(1 - e^{-1})(1 - \cos(1)). \end{aligned} \tag{22}$$

To compute this integral numerically, we introduce a computational domain based on the coordinates

$$\xi = \frac{x^2 - y^2 - 1}{3}, \quad \text{and} \quad \eta = \frac{xy - 1}{2}.$$

For a given $n \in \{16, 32, 64, 128, 256, 512\}$, we divide ξ and η uniformly into $n + 1$ points to produce a Cartesian grid on the square $\Omega_\xi = [0, 1]^2$. The physical coordinates x and y are

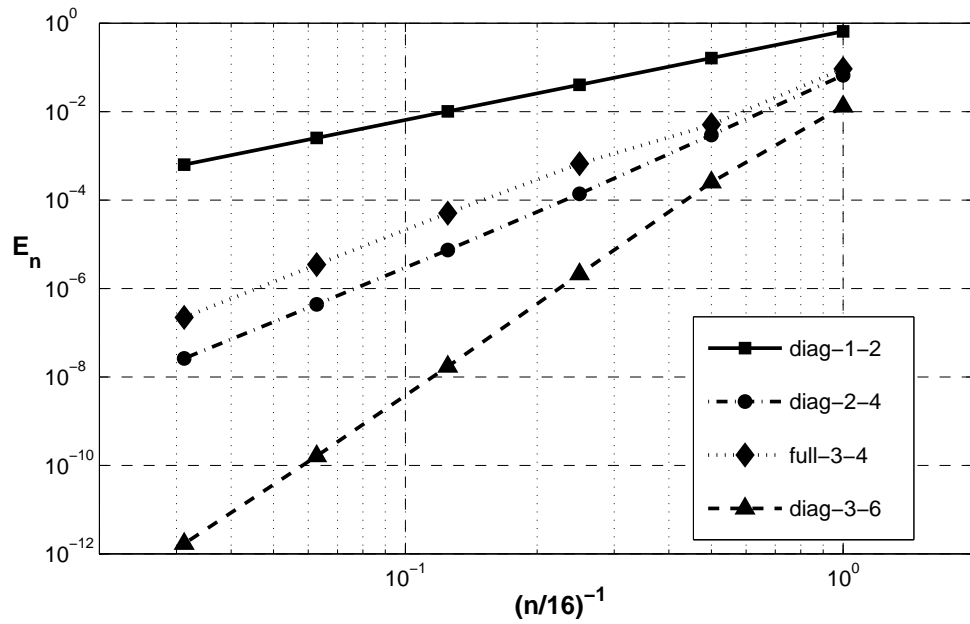


Figure 1: Errors of the SBP-based quadrature rules applied to (20).

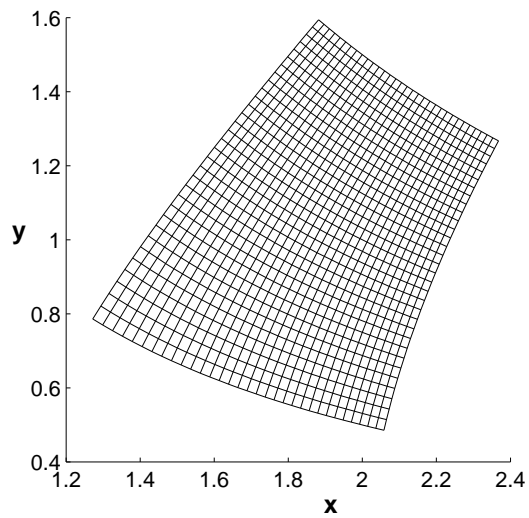


Figure 2: Example grid for Ω_x with $n = 32$.

evaluated at each computational coordinate, and these are used to compute the integrand in (22), which we denote by f . The grid for $n = 32$ is shown in Figure 2.

The Jacobian of the transformation is approximated using

$$J = [(I \otimes D)x] \circ [(D \otimes I)y] - [(I \otimes D)y] \circ [(D \otimes I)x], \quad (23)$$

where \circ denotes the Hadamard product (the entry-wise product, analogous to matrix addition). We have assumed that the nodes are ordered first by ξ and then by η , so we can construct the two-dimensional derivative operators using Kronecker products of the one-dimensional operator D and identity matrix I .

For a given n , the SBP-based approximation of (22) is given by

$$\mathcal{I}_n = J^T(H \otimes H)f, \quad (24)$$

and the error in the quadrature is $E_n = \mathcal{I} - \mathcal{I}_n$. As before, the order of convergence for $n > 16$ is estimated by q_n given by (21). Figure 3 plots E_n and Table 3 lists q_n for the diagonal-norm SBP operators listed in Table 1. Despite their s -order accurate boundary closures, Table 3 confirms the theory and shows that the quadrature for the diagonal weight matrices remains $2s$ -order accurate. Note that the errors for the diag-3-6 scheme are corrupted by round-off error for $n = 256$ and $n = 512$, which explains the suboptimal values of q_n for these grids.

We have also included results for a mixed scheme in Table 3 and Figure 3. This mixed scheme uses the diag-3-6 SBP operator to evaluate the derivatives in the Jacobian (23) and the diag-2-4 operator to evaluate the quadrature (24). The results show that the mixed scheme has an asymptotic convergence rate of only 3. Thus, despite a more accurate approximation of the Jacobian, the mixed scheme produces a less accurate \mathcal{I}_n than the scheme using the diag-2-4 operator for both the Jacobian and quadrature. This illustrates the importance of using the same operator to obtain the theoretical convergence rate.

4.3. Discrete Divergence Theorem

We will now verify that diagonal-norm SBP operators mimic the divergence theorem accurately. Specifically, we wish to show that when the divergence of a vector field is discretized

Table 3: Rates of convergence for the diagonal-norm SBP operator approximation of (22).

SBP operator	n				
	32	64	128	256	512
diag-1-2	2.0911	2.0453	2.0226	2.0113	2.0056
diag-2-4	4.3283	4.1583	4.0768	4.0374	4.0093
diag-3-6	7.0799	6.7941	6.2253	2.1274	-0.7390
mixed	3.3170	2.0521	2.7215	2.8863	2.9484

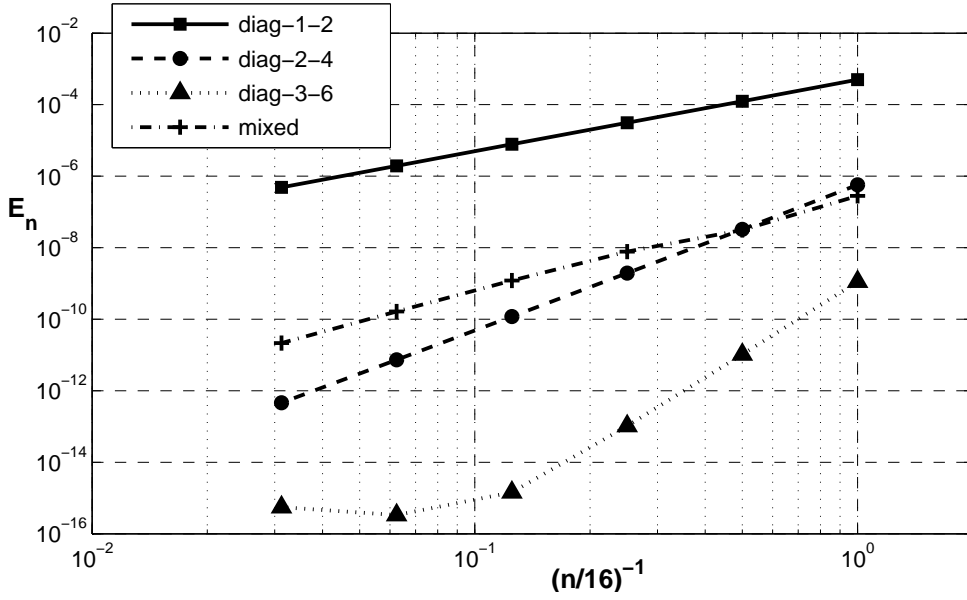


Figure 3: Errors of the SBP-based quadrature rules in approximating (22).

using SBP operators and then integrated using the corresponding SBP quadrature rule, the result depends only on the nodes along the boundary and is a $2s$ -order approximation to the surface flux.

We adopt the same domain Ω_x and coordinate transformation as in the previous example. A vector field $(\mathcal{F}, \mathcal{G})$ is defined by

$$\begin{aligned}\mathcal{F}(x, y) &= \frac{x}{2} \exp\left(\frac{1-xy}{2}\right) \cos\left(\frac{2\pi(x^2-y^2-1)}{3}\right) + \frac{2y}{3} \left(\frac{xy-1}{2}\right)^7 \sin\left(\frac{\pi(x^2-y^2-1)}{3}\right) \\ \mathcal{G}(x, y) &= -\frac{y}{2} \exp\left(\frac{1-xy}{2}\right) \cos\left(\frac{2\pi(x^2-y^2-1)}{3}\right) + \frac{2x}{3} \left(\frac{xy-1}{2}\right)^7 \sin\left(\frac{\pi(x^2-y^2-1)}{3}\right).\end{aligned}$$

The analytical value of the divergence of $(\mathcal{F}, \mathcal{G})$ integrated over the domain Ω_x is

$$\mathcal{I} = \iint_{\Omega_x} \frac{\partial \mathcal{F}}{\partial x} + \frac{\partial \mathcal{G}}{\partial y} dx dy = \frac{2}{\pi}. \quad (25)$$

The discrete divergence is evaluated in computational space using approximations for $\hat{\mathcal{F}}$ and $\hat{\mathcal{G}}$. In particular, the derivatives of the spatial coordinates that appear in (16) and (17) are approximated using SBP operators. Therefore, at the nodes, $\hat{\mathcal{F}}$ and $\hat{\mathcal{G}}$ take on the values

$$\begin{aligned}\hat{f} &= [(D \otimes I)y] \circ f - [(D \otimes I)x] \circ g, \\ \hat{g} &= -[(I \otimes D)y] \circ f + [(I \otimes D)x] \circ g,\end{aligned}$$

where f and g denote the values of \mathcal{F} and \mathcal{G} evaluated at the nodes.

The SBP approximation of \mathcal{I} is given by (see (15))

$$\mathcal{I}_n = c^T (H \otimes H) \left[(I \otimes D) \hat{f} + (D \otimes I) \hat{g} \right].$$

Table 4 lists the estimated order of accuracy q_n based on $E_n = \mathcal{I} - \mathcal{I}_n$ for the three diagonal-norm SBP operators diag-1-2, diag-2-4, and diag-3-6. As predicted, the SBP discrete divergence integrated using $(H \otimes H)$ is a $2s$ -order accurate approximation to \mathcal{I} . Moreover, in light of (19), we know that \mathcal{I}_n depends only on the boundary nodes (This has been confirmed by calculating the right-hand side of (19) and showing that it equals \mathcal{I}_n to machine error).

Table 4: Rates of convergence for the diagonal-norm SBP operator approximation of an integrated divergence field. Round-off errors are contaminating the estimates for diag-3-6 with $n = 256$ and $n = 512$

SBP operator	n				
	32	64	128	256	512
diag-1-2	2.0909	2.0453	2.0226	2.0113	2.0056
diag-2-4	3.7201	3.7862	3.9000	3.9532	3.9758
diag-3-6	7.5935	7.2371	7.8361	5.0507	-2.1760

4.4. Superconvergent Functionals

In the introduction, we noted that many functionals of engineering interest are integrals that depend on the solution of a PDE. In addition, when the PDE is discretized using a high-order finite-difference scheme, many quadrature rules are available to compute such functionals. In this final example, we illustrate the advantage of using SBP quadrature when the discrete solution is obtained using a corresponding SBP discretization. We emphasize that this example is not intended to verify the present theory; the previous numerical examples were provided for verification. Instead, the following is intended to motivate the broader role and investigation of SBP quadrature in numerical simulation.

We consider the steady quasi-one-dimensional Euler equations, which model an inviscid flow in a duct of varying cross-sectional area $S(x)$:

$$\frac{\partial \mathcal{F}}{\partial x} - \mathcal{G} = 0, \quad \forall x \in \Omega_x = [0, 1] \quad (26)$$

where the flux and source are given by

$$\mathcal{F} = \begin{pmatrix} \rho u S \\ (\rho u^2 + p) S \\ u(e + p) S \end{pmatrix}, \quad \text{and} \quad \mathcal{G} = \begin{pmatrix} 0 \\ p \frac{dS}{dx} \\ 0 \end{pmatrix},$$

respectively. The flow variables sought are the density, ρ , momentum per unit volume, ρu , and energy per unit volume, e . The ideal gas law closes the system of equations and defines

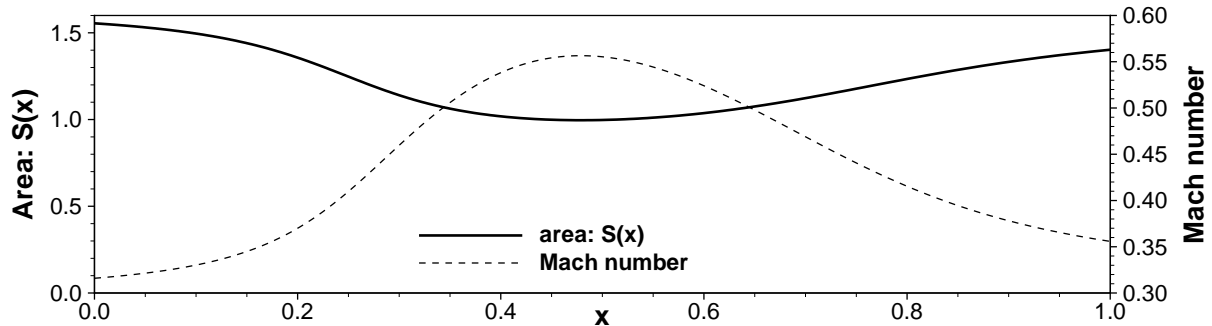


Figure 4: Duct area and Mach number for the quasi-one-dimensional-Euler flow example.

the pressure as

$$p = (\gamma - 1) \left(e - \frac{1}{2} \rho u^2 \right).$$

A constant specific heat ratio of $\gamma = 1.4$ is adopted. The flow variables are nondimensionalized using the inlet density and speed of sound. The x coordinate and area $S(x)$ and nondimensionalized based on the duct length.

We consider a converging-diverging duct defined by

$$S(x) = \frac{8}{5} - \frac{1}{\pi} [\arctan(8x - 2) + \arctan(3 - 4x)], \quad x \in [0, 1].$$

Figure 4 shows the variation of S along the length of the duct. For an isentropic flow, the exact solution is entirely determined by the ratio S/S^* , where S^* denotes the critical area where the Mach number is unity; see [9] for example. For the present example we set $S^* = 0.8$, ensuring that the flow remains subsonic over the entire domain. The analytical Mach number variation based on $S(x)$ and S^* is plotted in Figure 4.

Equation (26) is discretized on a nonuniform mesh based on the coordinate transformation

$$x(\xi) = \frac{e^{4\xi} - 1}{e^4 - 1}, \quad \xi \in [0, 1],$$

where the computational coordinate ξ is discretized uniformly. The coordinate transformation does not change the form of the steady quasi-one-dimensional Euler equations; however, the transformation does introduce a metric Jacobian into integral functionals on Ω_x .

The derivatives appearing in (26) are discretized using diagonal-norm SBP operators, and boundary conditions are imposed weakly using simultaneous approximation terms (SATs) [1, 3]. The exact solution is used to provide boundary data to the SAT penalties at $x = 0$ and $x = 1$. Stable artificial dissipation [11] is introduced to damp high-frequency oscillations. The unknowns are ordered first by flow variable and then by node, i.e., the solution vector has the form

$$q^T = \left[(\rho, \rho u, e)_0, (\rho, \rho u, e)_1, \dots, (\rho, \rho u, e)_n \right];$$

hence, the discretized Euler equations can be written as

$$(D \otimes I_3) f + \nu (H^{-1} M \otimes I_3) q - g = - (H^{-1} \otimes I_3) \Sigma (q - q_{bc}), \quad (27)$$

where $D = H^{-1}Q$ is the diagonal-norm SBP operator on $n + 1$ nodes, I_3 is the 3×3 identity matrix, and M is a symmetric positive semi-definite dissipation operator whose accuracy is consistent with D [11]. The dissipation operator is scaled by the constant $\nu = 0.04$ for all cases considered below. The vectors f and $g \in \mathbb{R}^{3(n+1)}$ denote the flux and source terms evaluated at each node, respectively. The block diagonal matrix Σ determines the appropriate penalties based on the incoming characteristics. Specifically,

$$\Sigma = \text{diag} (A^+, 0, 0, \dots, -A^-),$$

where $A^+ \in \mathbb{R}^{3 \times 3}$ (resp. A^-) denotes the flux Jacobian $A = (\partial \mathcal{F} / \partial \rho \quad \partial \mathcal{F} / \partial \rho u \quad \partial \mathcal{F} / \partial e)$ with negative (resp. positive) eigenvalues set to zero. The vector q_{bc} denotes the exact solution evaluated on the mesh.

To verify the discretization accuracy, Equation (27) is solved on a sequence of meshes with $n = 16, 32, 64, 128, 256$, and 512 nodes. Table 5 lists the estimated convergence rate in the L_∞ -norm of the Mach-number error for the solutions corresponding to the SBP operators diag-1-2, diag-2-4, and diag-3-6. Asymptotically, the solution errors appear to be one degree higher than their corresponding boundary-closure accuracy, which is consistent with theoretical predictions [4].

Next we consider the question of interest: what is the advantage of using SBP quadrature for integral functionals that depend on the solution of a discretized PDE? Consider the

Table 5: Convergence rates in the L_∞ norm of the Mach-number error for solutions to the discrete Euler equation (27).

SBP operator	n				
	32	64	128	256	512
diag-1-2	1.9192	2.7364	2.1597	2.0422	2.0175
diag-2-4	3.7768	4.4711	3.0734	2.8005	2.9401
diag-3-6	3.2718	3.3455	5.1085	4.8276	4.5698

integral of kinetic energy over the domain $\Omega_x = [0, 1]$.

$$\mathcal{K} \equiv \int_0^1 \frac{1}{2} \rho u^2 dx = \int_0^1 \frac{1}{2} \rho u^2 \frac{\partial x}{\partial \xi} d\xi.$$

We will approximate this integral using SBP quadrature and *the discrete solution* of (27). Thus, on the mesh with $n + 1$ nodes the approximate functional is given by

$$\mathcal{K}_n = J^T H k,$$

where $k \in \mathbb{R}^{n+1}$ is a vector consisting of the kinetic energy at each node, and $J = Dx$ is an approximation to the Jacobian of the transformation. The exact value of \mathcal{K} is estimated using the composite Simpson's rule on a uniform mesh with $n = 2048$ intervals, i.e., 4 times greater resolution than the finest mesh considered.

Table 6 lists the convergence rates of \mathcal{K}_n . The functional convergence rates are consistent with the accuracy of the SBP quadrature rules, despite the lower accuracy of the discrete solution. This functional superconvergence is a consequence of using an SBP discretization for the PDE and the corresponding SBP quadrature for the functional; see [6] for additional details on the theory.

For comparison, Table 6 includes the results of applying Simpson's rule to the fourth-order accurate solution obtained from the diag-3-6 discretization. Using Simpson's rule, superconvergence is not observed and the functional remains asymptotically fourth-order accurate.

Table 6: Convergence rates for the total kinetic energy functional, \mathcal{K}_n , evaluated using solutions of the discretized Euler equation (27).

SBP operator	n				
	32	64	128	256	512
diag-1-2	2.5336	2.5140	2.3803	2.2413	2.1384
diag-2-4	3.0200	4.7041	4.7039	4.4507	4.2722
diag-3-6	4.5094	8.4483	5.2564	6.6077	6.6533
Simpson's (diag-3-6)	4.1658	8.6555	3.9176	3.8446	3.9276

5. Conclusions

We have shown that the weight matrices of SBP finite-difference operators are related to trapezoid rules with end corrections. The result has significant implications for diagonal-norm SBP discretizations of PDEs, including the following.

- The diagonal-norm SBP energy norm, which is frequently used in the stability analysis of SBP-based PDE discretizations, is a $O(h^{2s})$ accurate approximation of the L^2 norm for functions on $[0, 1]$.
- The summation-by-parts property, equation (1), is a formal *and* accurate representation of integration by parts, equation (2). More generally, multi-dimensional diagonal-norm SBP discretizations using Kronecker products mimic the divergence theorem, i.e. the weight-matrix quadrature applied to the discrete divergence produces an accurate quadrature of the flux over the domain boundary in which no interior points are involved.
- Diagonal-norm SBP operators have s order-accurate boundary closures when the interior scheme is $2s$ -order accurate. This limits numerical PDE solutions to $s + 1$ order accuracy [4]; however, a diagonal-norm SBP discretization can produce superconvergent $2s$ -order-accurate functionals, if the corresponding SBP quadrature rule is used to calculate the functional [6].

In light of these observations, the SBP weight matrix appears to be the natural quadrature rule for evaluating functionals from corresponding diagonal-norm SBP discretizations.

We have not considered the impact of curvilinear transformations on quadratures based on full and restricted-full norms. Numerical experiments suggest that these quadratures also remain accurate on transformed domains, but further analysis is necessary to prove this hypothesis. This will be the focus of future work.

References

- [1] M. H. Carpenter, D. Gottlieb, S. Abarbanel, Time-stable boundary conditions for finite-difference schemes solving hyperbolic systems: methodology and application to high-order compact schemes, *Journal of Computational Physics* 111 (2) (1994) 220–236.
- [2] P. Diener, E. N. Dorband, E. Schnetter, M. Tiglio, Optimized high-order derivative and dissipation operators satisfying summation by parts, and applications in three-dimensional multi-block evolutions, *Journal of Scientific Computing* 32 (1) (2007) 109–145.
- [3] D. Funaro, D. Gottlieb, A new method of imposing boundary conditions in pseudospectral approximations of hyperbolic equations, *Mathematics of Computation* 51 (184) (1988) 599–613.
- [4] B. Gustafsson, The convergence rate for difference approximations to mixed initial boundary value problems, *Mathematics of Computation* 29 (130) (1975) 396–406.
- [5] J. E. Hicken, D. W. Zingg, A parallel Newton-Krylov solver for the Euler equations discretized using simultaneous approximation terms, *AIAA Journal* 46 (11) (2008) 2773–2786.
- [6] J. E. Hicken, D. W. Zingg, Superconvergent functional estimates from summation-by-parts finite-difference discretizations, *SIAM Journal on Scientific Computing* 33 (2) (2011) 893–922.
- [7] F. B. Hildebrand, *Introduction to Numerical Analysis*, 2nd ed., McGraw-Hill Inc., New York, NY, 1974.
- [8] H.-O. Kreiss, G. Scherer, Finite element and finite difference methods for hyperbolic partial differential equations, in: C. de Boor (ed.), *Mathematical Aspects of Finite Elements in Partial Differential Equations*, Mathematics Research Center, the University of Wisconsin, Academic Press, 1974.
- [9] A. M. Kuethe, C.-Y. Chow, *Foundations of Aerodynamics: Bases of Aerodynamic Design*, 4th ed., John Wiley & Sons, Inc., New York, NY, 1986.
- [10] J. Li, General explicit difference formulas for numerical differentiation, *Journal of Computational and Applied Mathematics* 183 (1) (2005) 29–52.
- [11] K. Mattsson, M. Svård, J. Nordström, Stable and accurate artificial dissipation, *Journal of Scientific Computing* 21 (1) (2004) 57–79.

- [12] K. Mattsson, M. Svärd, M. Shoeybi, Stable and accurate schemes for the compressible Navier-Stokes equations, *Journal of Computational Physics* 227 (4) (2008) 2293–2316.
- [13] J. Nordström, J. Gong, E. van der Weide, M. Svärd, A stable and conservative high order multi-block method for the compressible Navier-Stokes equations, *Journal of Computational Physics* 228 (24) (2009) 9020–9035.
- [14] M. Osusky, J. E. Hicken, D. W. Zingg, A parallel Newton-Krylov-Schur flow solver for the Navier-Stokes equations using the SBP-SAT approach, in: 48th AIAA Aerospace Sciences Meeting, No. AIAA–2010–0116, Orlando, Florida, 2010.
- [15] E. Pazos, M. Tiglio, M. D. Duez, L. E. Kidder, S. A. Teukolsky, Orbiting binary black hole evolutions with a multipatch high order finite-difference approach, *Physical Review D (Particles, Fields, Gravitation, and Cosmology)* 80 (2) (2009) 024027–1–024027–8.
URL <http://link.aps.org/abstract/PRD/v80/e024027>
- [16] T. H. Pulliam, J. L. Steger, Implicit finite-difference simulations of three-dimensional compressible flow, *AIAA Journal* 18 (2) (1980) 159–167.
- [17] B. Strand, Summation by parts for finite difference approximations for d/dx , *Journal of Computational Physics* 110 (1) (1994) 47–67.
- [18] M. Svärd, On coordinate transformations for summation-by-parts operators, *Journal of Scientific Computing* 20 (1) (2004) 29–42.
- [19] P. D. Thomas, C. K. Lombard, Geometric conservation law and its application to flow computations on moving grids, *AIAA Journal* 17 (10) (1979) 1030–1037.